Bioceramics Development and Applications

Maji and Dasgupta, Bioceram Dev Appl 2017, 7:2
DOI: 10.4172/2090-5025.1000103

Research Article Open Access

Effect of β-Tricalcium Phosphate Nanoparticles Additions on the Properties of Gelatin-Chitosan Scaffolds

Maji K and Dasgupta S*

Department of Ceramic Engineering, NIT, Rourkela, India

Abstract

Bone tissue engineering, using a synthetic porous scaffold material provides some distinct advantages over autografting and allografting, and it is a rapidly growing alternative approach to heal damaged bone tissue. The current study focuses on fabrication and characterization of nano β-TCP incorporated gelatin- chitosan based composite scaffold for bone regeneration at the sites of musculoskeletal defects and disorders.

Gelatin-chitosan scaffold reinforced with beta-tricalcium phosphate (β-TCP) nanopowder was fabricated through freeze drying of material's suspension. From powder X-ray diffraction and Fourier transform infrared spectrometer analysis the presence of phase pure β-TCP powders in gelatin-chitosan matrix was confirmed. Gelatin-Chitosan-β-TCP (GCT) scaffold exhibited a homogenouos porous structure with an average pore size of 118 ± 11 μm. Micro-CT image confirmed interconnected porous network with homogeneous distribution of β-TCP nanoparticles in Gelatin-Chitosan (GC) matrix. GCT scaffold showed higher compressive strength of 2.45 ± 0.15 MPa as compared to 1 MPa exhibited by neat GC scaffold. Protein adsorption capacity was increased to 22 mg/cc in GCT scaffold from 13 mg/cc in GC scaffold. Weight loss of GCT scaffold was lower of 26% as compared to 47% in GC scaffold after 8 weeks of incubation in phosphate buffer solution of pH 7.4. Mesenchymal stem cells cultured onto GCT scaffold exhibited higher degree of lamellipodia and filopodia extensions and greater spreading onto GCT scaffold as compared to that in GC scaffold after 7 and 14 days of culture. MTT assay suggested higher degree of proliferation of MSCs cultured onto GCT scaffold as compared to that onto pure GC scaffolds. This study demonstrates that β-TCP incorporation into gelatin- chitosan matrix improved osteogenic potential of the scaffold suitable for bone tissue engineering.

Keywords: Chitosan; Gelatin; β-TCP; Scaffold; Protein adsorption; Bioactivity

Introduction

The current challenges of using autografts [1] and allograft [2] have inspired the development of bone tissue engineering, in which synthetic or natural material can encourage the formation of new tissue by delivering appropriate cells into the host [3]. For this purpose, it is important to define an adequate material composition that will provide the mechanical support and an appropriate source of cells that will restore the tissue function.

Human mesenchymal stem cells have attracted considerable attention in bone tissue engineering due to its high osteogenic differentiation potential [4]. Recent study suggested that osteogenic differentiation of MSC's down to osteogenic pathway appear to be highly dependent on material composition [5]. It is very important to understand the cell-material interaction that will ultimately guide new tissue regeneration and prevent the formation of fibrous capsule.

Extracellular matrix of bone is an inorganic- organic hybrid comprised mainly of nano hydroxyapatite crystal in collagen fibril [4]. With this understanding, researchers have exploited ceramic and polymer composite biomaterial for use in bone tissue engineering [6]. Biopolymer-ceramic based porous scaffolds that promote new bone formation by recruiting osteogenic cells at the implantation site have attracted much attention to the researchers [7]. Biopolymers such as chitosan, alginate, gelatin are commonly used natural biopolymer reinforced with hydroxyapatite, β-tricalcium phosphate and biphasic calcium phosphate [8]. Chitosan (poly-1,4-d-glucosamine) is a partially deacelytated product from chitin [9], have been used in bone tissue engineering due to its structural similarity with glycosaminoglycan in extra cellular matrix of bone [10]. Gelatin, a partial derivative of collagen has many desirable properties such as excellent osteoconductivity, lack of antigenicity etc. useful for bone tissue engineering [11].

Because of excellent biocompatibility and biological characteristics that are similar to human bone, natural biopolymer and CaP based composites were investigated extensively. Agarose, alginate, silk, hyaluronic acid, collagen, chitosan, gelatin is some of the well known natural biopolymers that have been used for bone tissue engineering application. BCP (HA + β-TCP)/agarose macroporous scaffolds was studied using mouse L929 fibroblasts and human SAOS-2 osteoblasts during different colonization times [12]. Tampieri et al. studied porous [13-15] HA-alginate scaffold prepared using freeze drying technique that exhibited high degree of *in vitro* biocompatibility and controlled biodegradability. Osteoinductive properties of porous hybrid scaffolds prepared from β-TCP, alginate-gelatin was reported elsewhere [16]. Functionally graded HA/silk fibroin biocomposite prepared by pulse electric current sintering [17,18] showed excellent mechanical strength and osteoconductivity. Le et al. proposed that the physical, chemical and biological properties of calcium orthophosphate bioceramics and the fibrin glue might cumulate in biocomposites suitable for preparation of advanced bone grafts [19]. Gea et al. [20] prepared HAp/chitin composite with HAp content varying between 25% to 75% wt% and studied it *in vivo* bone regeneration ability in rat. Moreover, Lee et al. [21] proposed in their research the use of chitosan/TCP sponges

***Corresponding author:** Sudip Dasgupta, Assistant Professor, Department of Ceramic Engineering, National Institute of Technology, Rourkela, Odisha-769008, India, Tel: 919937565248; E-mail: gsudip02@yahoo.co.in

Received September 21, 2017; **Accepted** October 09, 2017; **Published** October 17, 2017

Citation: Maji K, Dasgupta S (2017) Effect of β-Tricalcium Phosphate Nanoparticles Additions on the Properties of Gelatin-Chitosan Scaffolds. Bioceram Dev Appl 7: 103. doi: 10.4172/2090-5025.1000103

as tissue engineering scaffolds for bone regeneration. Bioglass-chitosan composite also exhibited the potential to support the growth of osteoprecursor cells *in vitro* and to favour differentiation of osteoblast [22].

Further, Kartikasari et al. [23] studied hydroxyapatite reinforced gelatin-Chitosan scaffoldfor the treatment of bone defects and found hydroxyapatite promoted pre-osteoblast proliferation and matrix synthesis. Additionally, Hafezi et al. [24] investigated the effect ofnano bioglass associated with Gelatin matrix to induce repair ofosteochondral defects in rabbit. A porous gelatin-chitosan-β-TCP scaffold prepared by khan et al. demonstrated improved mechanical property and in vitro biocompatibility [25]. Moreover, gelatin-chitosan-β-TCP based scaffolds prepared by Serra et al. exhibited in vitro differentiation of Human Osteoblast Cell (HOB) and good antibacterial activity which prevented them from risk of inflammatory response [26]. However, no study has yet been performed to study the effect of b-TCP nanoparticles on microstructure, protein adsorption capacity and biodegradability of gelatin- chitosan- b TCP based scaffold. Keeping this in view, here we reported the effect of incorporation of β-TCP nanoparticles on microstructure, protein absorption, biodegradation characteristics of prepared gelatin-chitosan based scaffolds. The effect of addition of nano hydroxyapatite particles into gelatin chitosan based scaffold has been reported in our earlier study [27].

In the current study, β-TCP nanoparticles to the extent of 30 wt% were incorporated into gelatin-chitosan matrix and cross-linked with glutaraldehyde to prepare 3D porous scaffolds. Microstructure and pore size distribution in the scaffold were analysed using SEM and micro CT. The interaction between human umbilical cord derived mesenchymal stem cells (HUMSCs) and the prepared scaffolds were investigated using SEM, MTT assay. As a whole, this study focused on exploring the effect of addition of β-TCP nanoparticle on mechanical strength, biodegradability, protein adsorption capacity and bioactivity of gelatin-chitosan scaffolds to enhance its bone regeneration potential at the implanted site.

Materials and Method

Calcium nitrate tetrahydrate ($Ca(NO_3)_2$,$4H_2O$), Diammonium hydrogen phosphate ($(NH_4)_2HPO_4$), Ammonium hydroxide (NH_4OH), Gelatin (type B, from bovine skin), and Chitosan (degree of deacetylation >85%) powder was procured from Sigma-Aldrich (St. Louis, MO). Glacial acetic acid was purchased from Himedia, India. phosphate buffer saline (PBS) and Dulbecco's modified eagle medium (DMEM) were procured from Invitrogen. BSA was obtained from Merck, India.

Fabrication of gelatin-chitosan-β-TCP scaffold

The gelatin-chitosan-β-TCP (GCT) composite scaffold was prepared according to our previous work [28]. Desired amount of chitosan (medium molecular weight and deacetylation degree ≈85%) was dissolved overnight in acetic acid (1% v: v) to obtain a chitosan solution (2% wt). Afterwards, gelatin (4 wt%) solution was mixed with chitosan solution and stirred at 500 rpm for 3 h. 30 wt% β-TCP nanoparticles were added to gelatin-chitosan solution to adjust the weight ratio of gelatin/ chitosan/β-TCP as 30:40:30. Afterward, the mixture was kept stirring for 2 h under ambient condition until the powders were thoroughly dispersed in the slurry. 0.25% of glutaraldehyde solution was added to slurry for crosslinking of gelatin-chitosan matrix followed by freezing at -20°C overnight. Finally, the scaffolds were kept in the freeze drier at -52°C for 72 hours (Figure 1). The scaffold was immersed in 5 wt% sodium borohydride followed by 10 wt% NaOH solution for 2 h to remove excess glutaraldehye and acetic acid, washed with deionized water and freeze dried.

Characterization

Physico-chemical characterization of gelatin/chitosan/β-TCP scaffold

XRD and FT-IR analysis were performed for evaluation of phases and chemical groups present in the prepared scaffolds. XRD analysis of the prepared scaffolds was performed with X-ray diffractometer (Panalytical, USA), using Cu Kα wavelength at 40 kV and 30 mA. FTIR analysis of all the prepared scaffolds were performed by using KBr pellets method. Microstructure of the prepared scaffolds was analysed using SEM (FEI, Nova-Nano 450, Nederland) operated at 78 A, 15 KV. Pore diameters of ternary composite scaffold were studied on the basis of FE-SEM images.

Apparent porosity of scaffold

The porosity of composite scaffold was measured using Archimedes principle with xylene as liquid medium using the following equation [29].

$$Porosity(\%) = \frac{w_2 - w_1}{w_2 - w_3} \times 100$$

Where W_1 is the weight of the sample in air, W_2 is the weight of the soaked sample with liquid in pores, and W_3 is the weight of the sample suspended in xylene. Dry weight of all freeze-dried scaffolds was taken accurately using a digital balance. Scaffold with a defined shape kept inside a beaker filled with ethanol and placed this beaker inside a vacuum desiccator to remove entrapped air present inside the scaffold.

Micro-tomography

GCT scaffolds (n=3) were scanned using micro-Computed Tomography (micro-CT) for microstructural characterization. For tomography experiment, the detector was placed at 450 μm away from the sample stage. The sample was rotated in steps of (0.2°) and was exposed to a beam energy (E=28 keV) for a duration of 5 seconds for all the samples. Data sets were reconstructed with in house developed

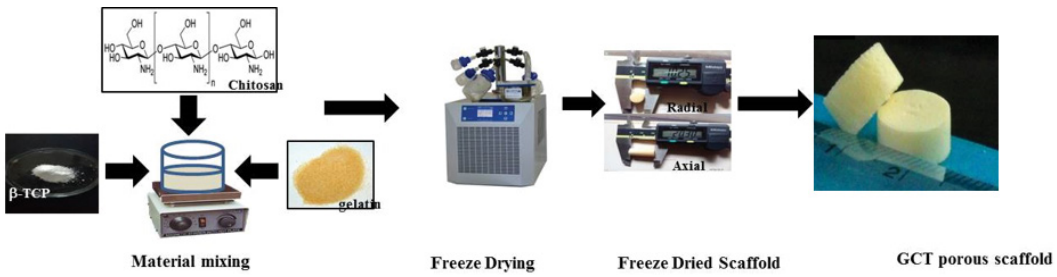

Figure 1: Schematic of fabrication of GCT scaffold using lyophilizing method.

software based on cone-beam reconstruction using FDK method [30]. The scanned images were acquired at a pixel size of 11.4 μm. Total acquisition time was approximately 20 min and more than 900 2-D images were recorded for each sample. Representative data sets were segmented into binary images which were used for morphometric analysis and to build 3D virtual models. The morphometric analysis included porosity, scaffolds interconnectivity, mean pore size and respective distribution.

In-vitro degradation

The biodegradation study of the scaffold was carried out *in vitro* according to a previously described method [31]. In brief, pieces of sponges (3 cm × 3 cm × 3 cm) were immersed into phosphate-buffered saline (PBS) solution (pH=7.4) containing lysozyme upto 1 month. The scaffolds were taken out from the medium, at a predetermined day interval and washed with distilled water followed by freeze–drying of the samples. The degradability percentage of the scaffold was calculated as follows:

$$D = \frac{W_0 - W_t}{W_0} \times 100\%$$

Where W_o denotes the original weight and W_t is the weight at day t. Each biodegradation experiment was conducted on three samples and the average value was taken as the percentage of biodegradation.

Protein adsorption

The protein absorption studies were carried out for the prepared scaffold upto 4 week in PBS. The samples were cut in equal weight and size and kept immersed in PBS with serum proteins for the respective time periods. BSA protein was dissolved in PBS at pH 7.4 to give a final concentration of 0.5 mg/ml. Scaffolds were cut into circular cube specimens, of which each side was 2 mm.

The scaffolds were immersed in PBS solution overnight prior to adsorption. Afterwards, scaffolds were dipped in 5 ml protein solution and incubated at 37°C for 24 h. The amount of protein adsorbed on the substrates was determined by the micro-BCA protein assay. The protein absorption was then quantified by measuring the absorbance at 562 nm in a plate reader (BioTEK). The amount of adsorbed protein was determined after comparing the absorbance of the samples with a calibration curve. Three repetitions were performed for all samples.

Mechanical properties

The compressive strength of the scaffolds was measured using a Universal Testing Machine (Tinius Olsen, UK) equipped with a load cell of 1 KN at a constant rate of 1 mm min^{-1} at room temperature. To evaluate mechanical properties of the scaffolds in the wet state, samples were immersed in the distilled water for 24 h prior to testing. Cylindrical scaffolds were compressed at a constant cross-head speed of 1 mm/min. Compression tests were performed on the dry samples having dimensions Ø=8 cm and h=14 cm at a rate of 1 mm/min. The slope of the linear region in the stress–strain curve gave the compressive modulus values. Three independent repetitive experiments were performed on each sample.

In-vitro study

Cell attachment: Human Umbilical cord (UCB) derived MSCs were used for *in vitro* cell culture. The UCB MSCs were collected from Ispat General Hospital, Rourkela, India with prior consent from patient. The details of isolation and characterization can be obtained from the earlier research work in the Department of Biotechnology and Medical Engineering, NIT, Rourkela, India [32]. Before cell culture, prepared scaffolds were sterilized with 70% ethanol for 10 min. Then, MSCs were suspended in 500 L DMEM medium and were placed with a cell density of 100,000 cells/cm^2 on the top surfaces of the scaffold located in wells of 12-well culture plate. The cultures were then provided with DMEM medium containing 10 U/mL penicillin, and 10 U streptomycin and incubated in an atmosphere of 5% CO_2 and temperature of 37°C for a period of 14 days. MSCs-cultured scaffolds were fixed in 2.5% glutaraldehyde at 48°C for 24 h, followed by washing with PBS (phosphate buffer solution). The samples were then dehydrated sequentially with increasing concentration of ethanol (including 30, 50, 80, and 100%), coated with gold and visualized at an accelerating voltage using a Nova Nano scanning electron microscope.

Cell proliferation (MTT): MSCs proliferation onto prepared scaffolds was analysed using MTT assay. Briefly, MSC cultured scaffolds were transferred into new 24-well plates containing media and MTT solution (5 mg/mL in PBS) and incubated for 2 h at 37°C. After removing the culture media, 0.5 mL of extraction solution (dimethylsulfoxide: DMSO) was added into the scaffolds. Formazan crystals were dissolved into DMSO and turned the solution red. The absorbance of the supernatant was measured with a microplate reader (Perkin Elmer, USA) at 540 nm.

Statistical analysis

Quantitative data were obtained in triplicate (n=3) and reported as the mean ± standard deviation. Statistical analysis was performed using Student's t-test, a p value less than 0.05 was considered statistically significant.

Results and Discussion

XRD analysis

Figure 2 represents the XRD pattern of GC and GCT composite scaffold. Low intensity peaks of chitosan could be detected in GC scaffold while gleatin peaks were supressed. On the contrary, signature peaks of chitosan could not be detected in XRD of GCT due to the high intensity peak of highly crystalline β-TCP nanopowders. Characteristic diffraction peaks at 2θ=16.9, 25.7, 27.7, 30.9, and 34.3°, corresponding to the rhombohedral β-TCP crystal planes of (110)), (1010), (214), (0210), and (220) could be observed in GCT scaffold and was confirmed from JCPDS: 09169.

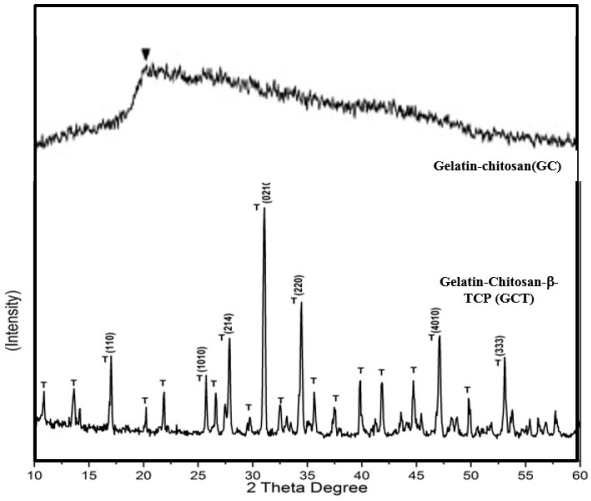

Figure 2: X-Ray diffraction pattern of gelatin/chitosan (GC) and gelatin/chitosan/-TCP(GCT) composite scaffold.

FTIR analysis

FTIR spectroscopy was performed to characterize the functional groups of gelatin, chitosan and GCT composite scaffold (Figure 3). Phosphate stretching and bending vibrations were observed at 506, 607, 1090, 1029 cm^{-1} in GCT scaffold signifies the presence of b- tricalcium phosphate phase in the scaffold [33]. Characteristic C=O stretching (amide I) at 1640 cm-1, N–H bending (amide II) at 1543 cm-1 were detected in GCT scaffold due to the presence of geletin [34]. The band at 3442 cm^{-1} and 1378 cm^{-1} confirms the presence characteristic –OH stretching vibration and C–H bending in chitosan [35]. Also, the formation of a chemical bond between Ca^{2}+ ions from β-TCP and the carboxyl group from the gelatin was detected at 1337 cm^{-1} that confirmed the interaction between bioceramic phase and gelatin matrix in GCT scaffold. The presence of characteristic C=N bond in GCT scaffold resulted due to gelatin-chitosan and intergelatin cross linking on reacting with glutaraldehyde could be observed at 1635 cm^{-1} that merged with the absorption band originated due to amide-I present in gelatin. In GCT composite scaffold, all the characteristic bands of gelatin, chitosan and β-TCP were observed indicated the presence of all three components in the scaffold.

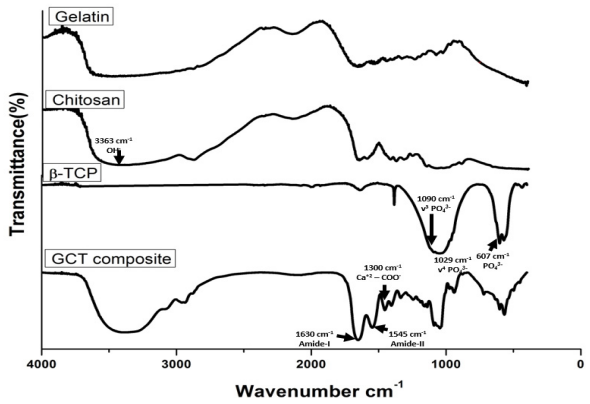

Figure 3: FTIR spectra of the prepared scaffold fabricated using freeze drying method.

Samples	Porosity (%)	Pore size (μm)
GC	85	188 ± 23
GCT	82	118 ± 12.6

Table 1: Porosity data of the fabricated scaffolds.

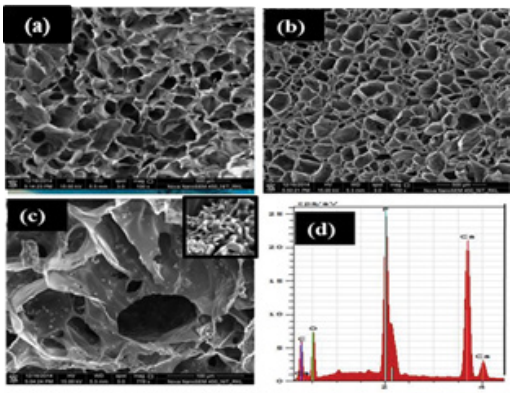

Figure 4: (a) SEM of three-dimensional GC scaffold prepared by freeze-drying technique, (b) Scanning electron micrographs of GCT scaffold, (c) Fracture surface of GCT scaffold, inset is higher magnification of pore wall showing -TCP particle, (d) EDS area analysis of GCT scaffold.

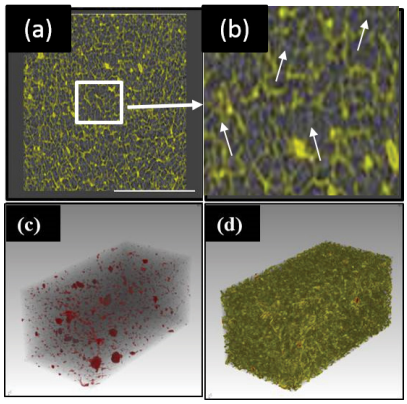

Figure 5: X-ray tomography showing 2D and 3D images of GCT scaffold (a) longitudinal section (scale bar 500 micron), (b) interconnected pores are shown by white arrow (c) TCP particle distribution inside GCT scaffold; (d) 3D reconstruction of the pore structure of the GCT scaffold showing homogeneity of the pores.

SEM analysis of prepared scaffolds

The microstructure of scaffolds plays a crucial role in bone tissue regeneration. Scaffolds must have an interconnected porous structure to allow adhesion, cellular proliferation and permeation of nutrients and oxygen [36]. The average pore size of GCT scaffold was lower of 118 ± 11 μm as compared that of 188 ± 23 μm in GC scaffold as depicted in Table 1. Transverse section of GCT scaffold Figures 4a and 4b showed high degree of porosity of 86.7 ± 0.9% with a mean pore size 118 ± 11 μm which has been reported to be suitable for cellular infiltration and exhibiting osteoinduction [37]. Fracture surface in Figure 4c of GCT scaffold showed interconnected porous network, where the β-TCP particles were homogeneously distributed on the pore wall (Figure 4c). Moreover, SEM -associated EDS area analysis of GCT scaffold revealed a Ca/P ratio of nearly 1.5 similar to that of β-TCP (Figure 4d).

Micro CT analysis of GCT composite scaffold

Micro-CT is a very useful, non-destructive tool that provides the architectural analysis of a scaffold used for tissue engineering before implantation [38]. Figures 5a and 5b) shows the representative photographs and 2D images of GCT scaffold using micro CT. Narrow pore size distribution with high degree of pore interconnectivity was observed in the prepared GCT scaffolds as shown in Figure 5b. Average pore size in the scaffold was found to be 107 ± 14 μm with a total porosity of 78% that corroborated well with the data obtained from SEM microstructure and Archimedes principle. It could be observed that the prepared scaffold possessed high porosity as well as pores were uniformly distributed in the horizontal and vertical sections of the scans, ideal for bone tissue ingrowth and exhibition of osteoinduction by the scaffold. The 3D spatial distribution of β-TCP particle (Figure 5c) throughout the scaffold confirmed the homogeneous distribution of nanoparticles into chitosan-gelatin matrix. This type of integration between particle phase and polymeric phase is due to the interaction between Ca^{2+} and COO- in gelatin and bio adhesive properties of chitosan [39]. The reconstructed 3D image in Figure 5d showed the porous structure and homogeneous distribution of pores throughout the GCT scaffold.

Degradation study

The degradation property of the prepared scaffolds with or without addition of β-TCP was assessed after incubating them in PBS of pH -7.4 for 4 weeks (Figure 6). GC scaffold registered a weight loss of

38% while that of GCT scaffold was significantly lower of 27% after 4 weeks of incubation in PBS. The degradation behavior of scaffold was mainly attributed to the hydrophilic groups of chitosan, gelatin, and their intermolecular bonding with β-TCP. Hydrophilic (amino, carboxilic) groups of gelatin and chitosanwere involved in electrostatic interactions with $Ca^{+2}$and $PO_4^{-3}$of β-TCP, and depressed the water uptake by the polymer netwrok, resulted in the decrease in degradation rate that is beneficial for making the scaffolled mechanically stable in *in vivo* condition. Degradation of the scaffolds must be controlled with a proper rate to match the speed of new tissues formation, that leads to proper wound haling [40].

Protein adsorption study

Protein adsorption is an important parameter as it determines cell adhesion onto the scaffold's surface. Figure 7 demonstrates the BSA adsorption efficiency of the prepared scaffold upto 6 days of incubation in protein solution. Protein adsorption rate on both GC and GCT scaffold got saturated after 36 hours of incubation. Results suggested that inclusion of nano β-TCP into the gelatin-chitosan scaffolds enhanced the protein adsorption capacity of the GCT scaffold as compared to pure GC scaffold. The exposed β-TCP nanoparticles in GCT scaffold surface increased the binding sites of proteins on material surface or enforced electrostatic interaction between the BSA and GCT surface and enhanced adsorption rate of proteins.

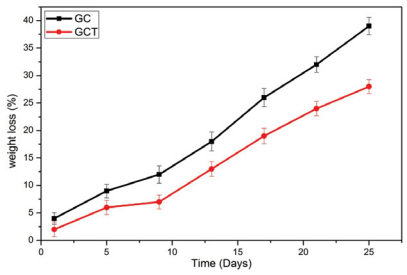

Figure 6: Degradation behaviour of GC and GCT scaffold after immersing them in PBS up to 4 weeks.

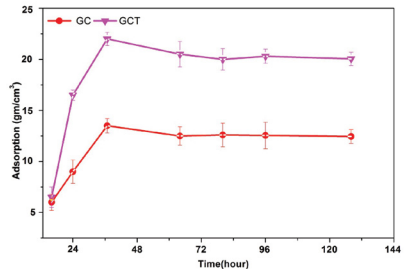

Figure 7: Protein adsorption on the scaffolds incubated with culture media for 6 days. Total protein adsorption was significantly high on composite scaffold. (*p<0.05).

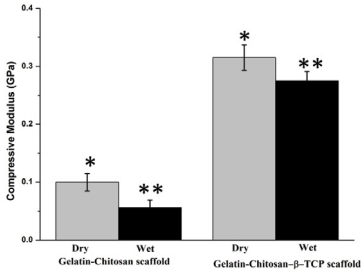

Figure 8: Mechanical properties of scaffold in dry and wet condition. (p*<0.5).

Sample	Compressive Modulus (GPa)		Compressive strength (MPa)
Cancellous Bone	0.05-0.5		12
Gelatin-Chitosan (control)	0.08 ± 0.09 (dry)	0.04 ± 0.03 (wet)	1
Gelatin-chitosan-b-TCP (GCT)	0.32 ± 0.06 (dry)	0.26 ± 0.03 (wet)	2.45

Table 2: Compressive modulus and strength data of GC and GCT scaffold.

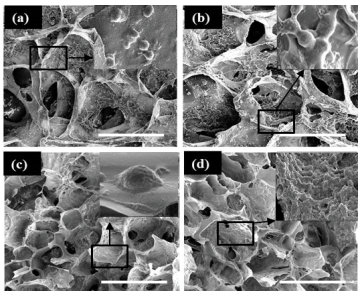

Figure 9: SEM images of cell attachment onto GC scaffold for (a) 7 days , (b) 14 days and GCT scaffold for (c) 7 days (d) 14 days.scale bar represents 100 micron.

Mechanical properties of prepared scaffolds

The scaffold used for bone regeneration is exposed to physiological fluid inside the body and hence it is important to evaluate its mechanical strength in wet state *in vitro***.** Compressive strength data of as prepared scaffolds as well as that immersed in PBS solution for 1 hour has been presented in Figure 8 and Table 2. Compressive strength of the scaffold also increased after incorporation of β-TCP nanoparticle from 1.1±0.13 MPa in GC scaffold to 2.45 ± 0.15 MPa in GCT scaffold. Moreover, compressive modulus of GCT scaffold was found to be significantly higher ($p<0.05$) as compared to that in pure GC scaffold both in wet and dry state. For cancellous bone, compressive strength and Young's modulus values are given in the range of 2–12 MPa and 0.05–0.5 GPa respectively [41] and the prepared GCT scaffold touched the lower limit of both compressive strength and modulus of cancellous bone. The reason for the increase in mechanical properties could be due to strong ionic interaction between Ca^{+2} in β-TCP with COO^- in gelatin and PO_4^{-3} in β-TCP with NH^{3+} in chitosan to strongly embed nanoceramic phase in gelatin- chitosan matrix that arrested and deflected crack propagation under the influence of stress. The mechanical properties of prepared GCT scaffolds were found to be significantly better than those of gelatin/chitosan scaffolds prepared by other groups using conventional methods [17].

Cell attachment study of prepared scaffolds using SEM

To evaluate the adhesion and growth of cell, we seeded and cultured MSCs on GCT scaffolds and GC scaffolds, and then examined MSC- scaffold interaction using SEM after 7 day and 14 days of culture. Figures 9a-9d showed that MSCs adhered and spread on surfaces of both GC and GCT scaffolds. At day 14 (Figures 9b and 9d), more number of cells were adhered to both the scaffolds as compared to that on after 7-day of cell culture (Figures 9a-9c). MSCs cultured onto GCT scaffold exhibited flatter morphology (Figure 9c inset) and higher number of lamellipodia, filopodia extensions onto scaffold as compared to the MSCs cultured onto GC scaffold (Figure 9a inset) which were round shaped after 7 days of cell culture. MSCs exhibited

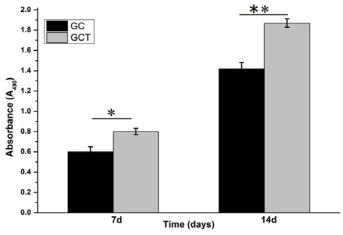

Figure 10: MTT assay of MSCs cultured onto GC and GCT scaffold after 7 days and 14 days of cell culture (*p<0.05, n=3).

higher spreading behaviour on GCT scaffold (Figure 9d) as compared to pure GC scaffold (Figure 9b) after cell culture time point of 14 days. The presence of β-TCP nanoparticles in GCT scaffolds offered higher number of points for focal adhesion through integrin mediated protein interaction between cultured MSCs and scaffolds [40]. These results suggested that β-TCP incorporated GCT scaffolds provided more conducive surface for MSCs adhesion, spreading and proliferation.

MTT assay

MTT assay indicates the ability of the scaffolds to provide ideal environment for cells cultured onto it to proliferate. The prepared scaffolds were cultured with MSC upto a period of 14 days. As evident from Figure 10 the cell density on both GC and GCT scaffolds were higher on 14 days as compared to that on 7 days suggesting the fact that both the scaffolds were supporting MSCs proliferation. Moreover, cell density on GCT scaffolds were found to be significantly higher (* and ** $p<0.05$) on 7 and 14 daysas compared that on pure GC scaffold. At all point of cell culture, GCT exhibited better capacity to proliferate MSC cultured onto it as compared to that by GC scaffold. Release of Ca^{+2} and PO_4^{3-} from GCT scaffolds played crucial role in enhancing its ability to proliferate MSCs better as compared to that by GC scaffold.

Conclusion

Highly porous gelatin- chitosan-β TCP based scaffolds were fabricated using freeze drying method. The prepared scaffolds had high degree of interconnected porosity and with addition of β-TCP nanoparticles the average porosity of gelatin- chitosan scaffolds was decreased to 118 mm that was sufficent for scaffolds to exhibit osteoinduction. β-TCP inclusion into gelatin-chitosan matrix improved compressive modulus and strength of the scaffold and enhanced its protein adsortion capability as compared to that by pure gelatin-chitosan scaffold. Biodegradability of gelatin-chitosan scaffolds decreased with incorporation of β-TCP nanoparticles. Mesenchymal stem cells cultured onto GCT scaffold exhibited better adhesion and spreding behavior as compared that onto pure gelatin-chitosan scaffold. MSCs cultured onto GCT scaffold exhibited higher degree of proliferation as compared that on pure gelatin chitosan scaffold. Thus β-TCP nanoparticle incorporation into gelatin –chitosan scaffold proved to be helpful in enhacing scaffold's mechanical strength, protein adsorption capacity and osteogenic potential for bone tissue engineering.

Acknowledgments

The authors would like to thank to Mr. Subhabrata Chakroborty from nit rourkela, for his help with the acquisition of SEM data, and to Dr. Asish Agarwal of RRCAT Indore, for the help in the m-CT analysis of the scaffolds. No funding sources to disclose. Authors are thankful to Ceramic Engineering Department for carrying out the experiment.

References

1. Bissada NF, Hangorsky U (1980) Alveolar bone induction. Dent Clin North Am 24: 739-749.
2. Mizutani A, Fujita T, Watanabe S, Sakakida K, Okada Y (1990) Experiments on antigenicity and osteogenicity in allotransplanted cancellous bone. Int Orthop 14: 243-248.
3. Aichelmann-Reidy ME, Yukna R (1998) Bone replacement grafts. The bone substitutes. Dent Clin North Am 42: 491-503.
4. Majumdar MK, Keane-Moore M, Buyaner D, Hardy WB, Moorman MA, et al. (2003) Characterization and functionality of cell surface molecules on human mesenchymal stem cells. J Biomed Sci 10: 228-241.
5. Murphy WL, Hsiong S, Richardson TP, Simmons CA, Mooney DJ (2005) Effects of a bone-like mineral film on phenotype of adult human mesenchymal stem cells *in vitro*. Biomaterials 26: 303-310.
6. Burg KJ, Porter S, Kellam JF (2000) Biomaterial developments for bone tissue engineering. Biomaterials 21: 2347-2359.
7. Rezwan K, Chen QZ, Blaker JJ, Boccaccini AR (2006) Biodegradable and bioactive porous polymer/inorganic composite scaffolds for bone tissue engineering. Biomaterials 27: 3413-3431.
8. Dorozhkin SV (2012) Biphasic, triphasic and multiphasic calcium orthophosphates. Acta Biomater 8:963-977.
9. Zhao F, Yin Y, Lu WW, Leong JC, Zhang W, et al. (2002) Preparation and histological evaluation of biomimetic three-dimensional hydroxyapatite/chitosan-gelatin network composite scaffolds. Biomaterials 23: 3227-3234.
10. Suh JK, Matthew HW (2000) Application of chitosan-based polysaccharide biomaterials in cartilage tissue engineering: a review. Biomaterials 21: 2589-2598.
11. Kim HW, Kim HE, Salih V (2005) Stimulation of osteoblast responses to biomimetic nanocomposites of gelatin–hydroxyapatite for tissue engineering scaffolds. Biomaterials 26: 5221-5230.
12. Sánchez-Salcedo S, Nieto A, Vallet-Regí M (2008) Hydroxyapatite/β-tricalcium phosphate/agarose macroporous scaffolds for bone tissue engineering. Chem Eng J 137: 62-71.
13. Tampieri A, Sandri M, Landi E, Biagini G (2005) HA/alginate hybrid composites prepared through bio-inspired nucleation. Acta Biomater 1: 343-351.
14. Gianluca T, Eleonora M, Francesca B, Sabrina S, Ivan D, et al. (2009) Alginate/hydroxyapatite biocomposite for bone ingrowth: A trabecular structure with high and isotropic connectivity. Biomacromolecules 10: 1575-1583.
15. Takeshi F, Takahisa A, Yoshitomo H, Yukari S, Hiroko K, et al. (2009) Octacalcium phosphate–precipitated alginate scaffold for bone regeneration. Tissue Eng Part A 15: 3525-3535.
16. Samavedi S, Whittington AR, Goldstein AS (2013) Calcium phosphate ceramics in bone tissue engineering: a review of properties and their influence on cell behavior. Acta Biomater 9: 8037-8045.
17. Miroiua FM, Socola G, Visana A, Stefana N, Craciun D, et al. (2010) Composite biocompatible hydroxyapatite–silk fibroin coatings for medical implants obtained by matrix assisted pulsed laser evaporation. Mater. Sci. Eng. B 169:151-158.
18. Bhumiratana S, Grayson W, Castaneda A, Rockwood D, Gil ES, et al. (2011) Nucleation and growth of mineralized bone matrix on silk-hydroxyapatite composite scaffolds. Biomaterials 32:2812-2820.
19. Le Guéhennec L, Layrolle P, Daculsi G (2004) A review of bioceramics and fibrin sealant. Eur Cell Mater 8: 11.
20. Yodsuwan N, Owatworakit A, Ngaokla A, Tawichai N, Soykeabkaew N (2012) Effect of carbon and nitrogen sources on bacterial cellulose production for bionanocomposite materials. in 1st Fah Luang University international conference, Thailand
21. Lee JY (2004) Transforming growth factor (TGF)-β1 releasing tricalcium phosphate/chitosan microgranules as bone substitutes. Pharm Res 21: 1790-1796.
22. Samira J, Hassane O, Mongi S, Fakhri K, Pellen P, et al. (2014) Cytocompatibility, gene-expression profiling, apoptotic, mechanical and 29Si, 31P solid-state nuclear magnetic resonance studies following treatment with a bioglass-chitosan composite. Biotechnol Lett 36: 2571-2579.
23. Yuliati A, Kartikasari N, Munadziroh E, Rianti D (2017) The profile of crosslinked bovine hydroxyapatite gelatin chitosan scaffolds with 0.25% Glutaraldehyde. J Int Dent Med 10: 151-155

24. Hafezi F, Nourani MR, Hossiennejad F, Mafi SM, Imani Fouladi AA (2012) Transplantation of nano-bioglass/gelatin scaffold in a non-autogenous setting for bone regeneration in a rabbit ulna. J Mater Sci Mater Med 23: 2783-2792.

25. Khan MN, Islam Jahid MM, Khan MA (2012) Fabrication and characterization of gelatin-based biocompatible porous composite scaffold for bone tissue engineering. J Biomed Mater Res A 100: 3020-3028.

26. Serra IR, Fradique R, Vallejo MC, Correia TR, Miguel SP, et al. (2015) Production and characterization of chitosan/gelatin/β-TCP scaffolds for improved bone tissue regeneration. Mater Sci Eng C 55: 592-604.

27. Maji K, Dasgupta S (2014) Hydroxyapatite-chitosan and gelatin based scaffold for bone tissue engineering. T Indian Ceram Soc 73: 110-114.

28. Maji K, Dasgupta S, Kundu B, Bissoyi A (2015) Development of gelatin-chitosan-hydroxyapatite based bioactive bone scaffold with controlled pore size and mechanical strength. J Biomater Sci Polym Ed 26: 1190-1209.

29. Maji K, Dasgupta S (2015) Bioactive glass and biopolymer based composite scaffold for bone regeneration. T Indian Ceram SoC 74:195-201.

30. Agrawal AK, Sarkar PS, Singh B, Kashyap YS, Rao PT, et al. (2016) Application of X-ray micro-CT for micro-structural characterization of APCVD deposited SiC coatings on graphite conduit. Appl Radiat Isot 108: 133-142.

31. Mao JS, Zhao LG, Yin YJ, Yao KD (2003) Structure and properties of bilayer chitosan–gelatin scaffolds. Biomaterials 24: 1067-1074.

32. Bissoyi A, Pramanik K (2014) Role of the apoptosis pathway in cryopreservation-induced cell death in mesenchymal stem cells derived from umbilical cord blood. Biopreserv Biobank 12: 246-254.

33. Gibson IR, Rehman I, Best SM, Bonfield W (2000) Characterization of the transformation from calcium-deficient apatite to β-tricalcium phosphate. J Mater Sci Mater Med 11: 799-804.

34. Meskinfam M, Sadjadi M, Jazdarreh H (2011) Biomimetic preparation of nano hydroxyapatite in gelatin-starch matrix. Eng Technol 52: 395-398.

35. Sharma C, Dinda AK, Mishra NC (2013) Fabrication and characterization of natural origin chitosan□gelatinalginate composite scaffold by foaming method without using surfactant. J Appl Polym Sci 127: 3228-3241.

36. Hutmacher DW (2000) Scaffolds in tissue engineering bone and cartilage. Biomaterials 21: 2529-2543.

37. Murphy CM, Haugh MG, O'Brien FJ (2010) The effect of mean pore size on cell attachment, proliferation and migration in collagen–glycosaminoglycan scaffolds for bone tissue engineering. Biomaterials 31: 461-466.

38. Hedberg EL, Kroese-Deutman HC, Shih CK, Lemoine JJ, Liebschner MA, et al. (2005) Methods: A comparative analysis of radiography, microcomputed tomography, and histology for bone tissue engineering. J Tissue Eng 11: 1356-1367.

39. Kim IY, Seo SJ, Moon HS, Yoo MK, Park IY, et al. (2008) Chitosan and its derivatives for tissue engineering applications. Biotechnol. Adv 26: 1-21.

40. Maji K, Dasgupta S, Pramanik K, Bissoyi A (2016) Preparation and evaluation of gelatin-chitosan-nanobioglass 3D porous scaffold for bone tissue engineering. Int J Biomater 2016:14.

41. Deligianni DD, Katsala ND, Koutsoukos PG, Missirlis YF (2000) Effect of surface roughness of hydroxyapatite on human bone marrow cell adhesion, proliferation, differentiation and detachment strength. Biomaterials 22: 87-96.